UCRL-JC-123312
PREPRINT

CONF-960163--29

Optical and Thermo-Optical Characterization of KTP and its Isomorphs for 1.06 μm pumped OPO's

RECEIVED
MAY 17 1996
OSTI

C. A. Ebbers
S. P. Velsko

This paper was prepared for submittal to the
SPIE 1996 Symposium on Lasers and Integrated Optoelectronics
San Jose, California
January 27-February 2, 1996

February 17, 1996

Lawrence Livermore National Laboratory

Optical and Thermo-Optical Characterization of KTP and its Isomorphs for 1.06 μm pumped OPO's

C.A. Ebbers and S.P. Velsko
Lawrence Livermore National Laboratory
Livermore, CA 94550 USA
Phone (510) 423-9465 Fax (510) 422-3361

Abstract

We have characterized the phasematching angle, linewidth, thermal conductivity, and $d\lambda/dT$ for KTP, KTA, and RTA optical parametric oscillators

---

* This work was performed under the auspices of the U.S. DOE by LLNL under contract no. W-7405-Eng-48.

Draft

Optical and Thermo-Optical Characterization of KTP and its Isomorphs for 1.06 μm pumped OPO's

C.A. Ebbers and S.P. Velsko
Lawrence Livermore National Laboratory
Livermore, CA 94550 USA
Phone (510) 423-9465 Fax (510) 422-3361

The need to protect personnel from inadvertent eye trauma from fielded laser sources dictates that the highest externally accessible fluences produced by these systems be kept below the maximum permissible exposure (MPE) for intra-beam viewing. The largest MPE value for a typical Q-switched (10 ns pulsewidth) source is 1 J/cm^2 for wavelengths in the range of 1.5 - 1.8 microns, while the MPE for a similar pulsewidth Nd:YAG source is 5 $\mu J/cm^2$.[1] This 5 order of magnitude difference in the MPE is one reason for the trend towards shifting the output of near infrared sources used for remote sensing or ranging to the "eyesafe" wavelength region, even at the expense of overall system efficiency. In addition to remaining within the 1500-1800 nm spectral region, a long range (>10 Km) remote sensing system would require that a significant fraction of the energy be contained within an atmospheric transmission window. Figure 1 shows the typical atmospheric transmission as a function of wavelength for a 50 Km slant path (3 Km to sea level) under STP and humidity conditions. (This spectral region is dominated by the vibrational overtone absorption of water and carbon dioxide.) Within the definition of the eyesafe wavelength region there are a number of high optical transmission windows with widths on the order of 1 nm. The widest window, indicated in Figure 1, is centered at 1555.5 nm and has FWHM of 1.3 nm.[2]

There are 5 nonlinear optical crystals available with apertures of at least 10x10 mm^2 which are also highly transparent in the 1.5 micron region; $LiNbO_3$, $KNbO_3$, KTP, KTA, and RTA. All 5 crystals are capable of 1555 nm generation in an orientation with a favorable nonlinear optical coupling. However, KTP, KTA, or RTA are preferred materials, given that the generated signal of the OPO should remain at a fixed wavelength, insensitive to angular or thermal variations. In Figure 2, the angle tuning of a 1.06 micron pumped KTP OPO relative to a $KNbO_3$ OPO is displayed. (The $d\lambda/d\theta$ of $LiNbO_3$ is of similar magnitude to that of $KNbO_3$.) The smaller angle tuning ($d\lambda/d\theta$) and smaller calculated thermal tuning ($d\lambda/dT$) of KTP relative to either $LiNbO_3$ or $KNbO_3$ implies that KTP or its isomorphs are the logical choice for implementation of an OPO centered at 1555.5 nm ± 0.25 nm. In addition, KTP has a damage threshold ~ 10x that of $LiNbO_3$, significantly reducing the need for aperture scaling of high pulse energy (>1 J/pulse) pumps.

The refractive indices and temperature derivatives can not be measured to sufficient accuracy to estimate $d\lambda/dT$ with a high degree of confidence. In addition, KTP is known to suffer from a non uniform birefringence across its aperture,[3] and the degree to which this might effect wavelength reproducibility from identically oriented crystals has not been previously examined. This paper is concerned with the effect of this nonuniform birefringence, as well as the angle and thermal tuning parameters for 1.064 micron pumped KTP, KTA, and RTA OPO's.

Thermal tuning of KTP, KTA, and RTA

An estimate of the change in wavelength with temperature, $d\lambda/dT$, derived from published dn/dT data for KTP[4] suggested that it might be possible to generate 1555 nm via noncritical phasematching, by operating at elevated temperature (> 100 °C). However, given the sensitivity of calculated $d\lambda/dT$'s to small errors in the individual dn/dT's, we directly measured $d\lambda/dT$ for X and Y cut, 1.064 micron pumped KTP and KTA OPO's. The crystals were mounted in a small, well insulated heater and the temperature was raised from room temperature to 150 °C and back again in 25 °C increments. The temperature was allowed to stabilize for ~ 15 minutes at each temperature setting. As seen in Table I, both KTP and KTA show a *decrease* in generated signal wavelength with increasing temperature. Moreover, of the available laser crystals from which high peak power, high average power has been generated ($YAlO_3$, YOS, YAG, and YLF), there is no suitable pump wavelength which will allow 1555 nm generation in a noncritically phasematched, X-cut KTP, KTA, or RTA oscillator (the orientation with largest Type II nonlinear optical coupling). While noncritically phasematched operation of a heated OPO is precluded (assuming the $d\lambda/dT$ of RTA is similar to that of KTP and KTA), a positive aspect of this result is that the thermal sensitivity of KTP is even less than expected.

The noncritical phasematched signal generated for a 1.06 μm pumped KTA (potassium titanyl arsenate) OPO is 1533 nm, while that of an RTA (rubidium...) OPO is 1671 nm. Thus, there is a possibility of growing a mixed KTA-RTA crystal that would be noncritically phasematched for 1555.5 nm generation. This would be accomplished by substituting ~14% rubidium for potassium in the KTA melt. (The same is true for YOS, YLF, or $YAlO_3$; each pump wavelength would require its own specific K/Rb ratio.) However, recent work[5] concerning the preferential incorporation of potassium in a KRTP (potassium rubidium titanyl phosphate) system, suggests that the high segregation coefficient observed in KRTP, may also be present in KRTA; a potential barrier to achieving large aperture crystals with uniform properties.

Table I. $d\lambda/dT$ for a 1.06 μm pumped X and Y cut KTP and KTA OPO

Crystal	X axis (nm/°C)	Y axis (nm/°C)
KTP	-0.022	-0.03
KTA	-0.014	a
RTA	-	a

[a]In process. Small nonlinear coupling makes OPO operation over sufficient time period difficult.

Wavelength of KTP, KTA, and RTA OPO's

KTP is known to suffer from a nonuniform birefringence,[3] leaving some uncertainty over how much the output wavelength would vary from crystal to crystal. Given that the OPO must be centered to within ±0.25 nm of 1555.5, direct measurements were made to accurately determine the magnitude of this variation in $\lambda(\theta \text{ or } \phi)$ for identically cut KTP and KTA crystals. It is also necessary to directly determine the absolute angle at which KTP is phasematched for 1555 nm generation, since the Sellmeier parameters for KTP[6] are derived from refractive index measurements determined only as far in the infrared as 1.5 μm. The Sellmeier parameters of KTA and RTA[7] are based on measurements taken further in the infrared (~4 μm) and should be of higher accuracy for infrared pumped OPO's.

The wavelength determination was made by directly measuring the generated signal in addition to measuring the sum frequency generated (SFG) wavelength produced by mixing of the 1.06 and 1.57 micron pump and signal. The direct measurement of the OPO output was measured using a 0.5 meter spectrometer. Calibration of the spectrometer was performed using three CW sources; He-Ne, Nd:YAG, and a 1523 nm source. The spectrometer was found to be linear and accurate to within ±0.1 nm (measured at each wavelength and multiple orders) over a 0.5 - 3 μm range. The spectrometer has a minimum step size of 0.2 nm, conservatively limiting the bandwidth determination of pulsed sources to < 0.6 nm FWHM. Nevertheless, this is of sufficient accuracy to determine whether the OPO bandwidth falls within the specified 1.3 nm wide window. The signal generated from each of the crystals was directed into the spectrometer and detected using an InGaAs photodiode. A second measurement method was also investigated, as it offered the possibility of a much more convenient and cost effective method for wavelength verification. It is based on the observation that when a single crystal (15-20 mm in length) is placed in a resonator with approximately an 80% reflectivity at the signal wavelength, oscillation of even an uncoated crystal can easily be observed. A second external KTP crystal is cut for sum frequency generation (SFG) of the pump and signal. This SFG signal was directed into an inexpensive 1/4 meter monochrometer and detected using a camera or a Si photodiode. An advantage of this method is that the output wavelength is near 634 nm (within 2 nm of the ubiquitous He-Ne source), allowing very accurate calibration of the monochrometer, and therefore accurate measurement of the generated SFG wavelength. In addition, the output is visible by eye, allowing the beam to be rapidly traced and aligned into the monochrometer. The measurement precision of the 1.55 micron signal, deduced from the SFG measurement, is reduced by a factor of 2 due to the weighting of the 1.06 μm in the SFG process. Nevertheless, the resources and time required for the SFG measurement are substantially reduced relative to the direct measurement.

The direct wavelength measurements are in good agreement with the SFG measurements, both of which are summarized in Table II. Figure 3 displays the calculated wavelengths generated for a 1.06 μm pumped KTP and RTA OPO for propagation in the X-Y (θ=90) plane, and for a KTA OPO for propagation in the X-Z (ϕ=0) plane. Good agreement between the measured wavelengths and the calculated wavelengths was observed for KTA and RTA. As expected, the largest discrepancy between calculated and measured signal wavelengths was observed for KTP.

The refractive indices of KTP can vary depending upon the flux, growth method, or the presence of impurities (such as Fe or Cr). Indeed, we measured a variation in output wavelength for X-cut KTP grown at separate facilities. However, at least in the case of two different manufacturers from which a number of identically cut KTP and KTA crystals were purchased, good reproducibility was observed. That is, *the signal wavelengths generated by identically cut crystals obtained from a single vendor were nearly identical.* Presumably, efficient use was made of the KTP or KTA boules, and several pieces were obtained from different locations in a single boule. This indicates that the position dependent refractive index variation that significantly affects the use of KTP as a compensated Q-switch,[3] is not significant enough to cause a substantial change in the output wavelength of the KTP crystals.

As calculated, a change in birefringence of 1×10^{-4} in the Z index will result in a 0.7 nm shift in the X-cut generated signal and a 0.5 nm shift in a Y-cut OPO. (Direct measurements of the refractive index variation in KTP have shown that the Z index variation in KTP is more than 10x larger than the X-Y variation.)[8] In X and Y-cut KTP, we have observed position dependent variations in the birefringence across the aperture of single crystals on the order of 1×10^{-04}/cm-1×10^{-05}/cm, dependent upon the manufacturer. In other recent work, a wavelength of 1571 nm was carefully measured from an X-cut, 1.064 μm pumped, KTP optical parametric oscillator.[9] The single crystal used for that work was obtained from Phillips, a vendor not represented in Table II . Given the magnitude of the birefringence variations observed in contiguous crystals in this work, it is conceivable that static birefringence variations of at least ~3×10^{-04} (producing a 2.1 nm shift in the generated signal for an X-cut OPO) can occur due to manufacturing differences in starting flux compositions, dopants, or growth temperatures, accounting for the observed shift in measured signals.

Table II. Measured wavelengths for various cut KTP, KTA, and RTA crystals

Crystal-Cut (θ,ϕ)	Calculated λ (nm)	Measured λ (Avg. nm)	Observed variation between samples	# Samples tested (Vendor)
KTP (90,0)	1571.1 nm	1574.9		1 - (A)
KTP (90,0)		1572.2	± 0.3 nm	5 - (B)
KTP (90,32)	1556 nm	1558.6	± 0.1 nm	5 - (B)
KTP (90,34)	1558	1556.2	± 0.1 nm	2 - (B)
KTP (90,90)	1520.6	1524.4	±0.4 nm	2 - (B)
KTA (90,0)	1533.2	1533.5	±0.2 nm	3 - (C)
KTA (78,0)	1548.9	1554.5		1 - (C)
RTA (90,90)	1543.6	1546.1		1 - (C)

Thermal conductivity and optical absorption

In KTP, optical absorption of the 3366 nm idler at average power operation will lead to the development of a thermally induced lens in the OPO crystals. Three parameters are needed to estimate the magnitude of the OPD at 1555 nm, the thermal conductivity, the optical absorption, and the dn/dT's. Only the thermal conductivity of KTP has been published,[6] no reference to the thermal conductivities of KTA or RTA were found. The thermal conductivities of KTP, KTA, and RTA were measured under contract at Cleveland Crystals Inc., and are displayed in Table III.

Table III. Thermal conductivity of KTP, KTA, and RTA

Crystals	κ_x (mW/cm-°C)	κ_y (mW/cm-°C)	κ_z (mW/cm-°C)
KTP	22	23	26
KTA	18	19	21
RTA	16	16	17

The estimated optical absorption for light polarized parallel to the Z axis (the polarization of the idler) is 35%/cm.[10] As seen in Figure 4,[11] the optical absorption of KTA in this wavelength region is significantly less (< 5%/cm). The difference in the thermally induced OPD for a KTP or KTA OPO can be estimated. We assume a 100 W pump (with negligible pump absorption), a pump depletion of 50%, and a 45 mm long path length OPO. The KTP OPO produces 33 W of 1555 nm light and 16 W of 3366 nm light. Using the standard model for the transverse temperature gradient in a cooled slab, the temperature rise from center to edge in the KTP crystal is calculated to be ~27 °C. The thermally induced OPD for this crystal length is ~ 6 waves, forming a positive focal length cylindrical lens, whereas the OPD in the KTA crystal of equivalent length is less than one wave. From a viewpoint of thermal lensing issues alone, KTA is a preferred crystal for a high average power operation.

Nonlinear Coupling

There is some controversy over the magnitude of the nonlinear optical coefficients of KTP, with values of d_{yzy} (relevant for X-cut noncritical phasematching in KTP) ranging from 3.3 to 2.65 pm/V. In addition, a recent measurement of the ratio of $d_{yzy}/d_{xzx} = 1.9$ has also been published.[12] In support of the latter ratio, we have observed operation of an X-cut KTP OPO well above threshold using a single, 20 mm long, X-cut KTP crystal. However, in the identical cavity under identical pump fluences, it is difficult to achieve threshold utilizing (2) 20 mm long Y-cut

KTP crystals. (Mirror reflectivities of the output coupler and high reflector were flat for the range between 1520 -1572 nm.) In effect, the nonlinear coupling for propagation near the Y axis of KTP, KTA, and RTA is effectively half that for propagation down the X axis.

Bandwidth Determination

Experience with average power frequency conversion of a diode pumped, Q-switched power oscillator[13] (100 mJ, 2.5 KHz, 25 ns) has demonstrated that long operating lifetimes can be obtained with average fluences of 1.5-2 J/cm^2 (4-5 peak) incident on dual AR (1.06/0.532 μm) coated KTP crystals. While the dual AR coatings for a KTP OPO (1.06/1.5555 μm) are not precisely identical to dual AR visible coatings (the coating is necessarily thicker due to the longer wavelength potentially leading to larger stresses in the coatings), this average fluence is presumed to be a point where safe operation of the OPO is possible.

We have characterized the performance of the resonator shown in Figure 5. This cavity consists of a 45^o input coupler, the antireflection coated KTP or KTA crystals, a dichroic beam splitter (high reflectivity@1555, high transmission@1064), and an output coupler (30-60%R). The 45^o input coupler serves several purposes. Although it adds substantially to the overall cavity length, it allows the pump collimation to be decoupled from the resonator optics, whose curvatures can be selected to form a stable, a marginal (flat-flat), or an unstable resonator. It adds a significant source of loss to the idler, reducing dual resonances. Finally, previous experience has shown that damage to the input coupler is much more likely to occur when the pump is directly transmitted through (as opposed to reflecting off of) the optic. The resonator, as configured in Figure 5, has the additional feature in that the pump and idler are cleanly separated from the signal, eliminating the need for additional prisms or filters to spectrally filter the signal.

In Figure 6, the energy and conversion efficiency of a 3 crystal (45 mm total length, (90,32) cut, 30% R@1555) KTP oscillator is displayed. Similar results were achieved with a 2 crystal (40 mm total length, X-cut KTA oscillator. Of particular importance is the measured bandwidth of the 2 or 3 crystal device. The largest aperture and length crystals currently available with moderate lead times is approximately 12x12x15 mm^3 for KTP, and 10x10x15 mm^3 for KTA. This implies that for large pulse energy sources (> 1 J/pulse), a 2-3 crystal resonator will be a necessity to meet the simultaneous requirements of a safe operating fluence and high energy conversion efficiency. The risk is that variations in the output wavelength from each crystal might require that each individual crystal be hand selected to produce the correct wavelength. However, as shown in Table II, the differential performance of the individual crystals was nearly within the measurement accuracy of the spectrometer. In any case, the measured bandwidth of the 3 crystal, critically cut KTP and the 2 crystal, noncritically cut KTA OPO was less than 0.6 nm FWHM, limited by the minimum step size of the spectrometer. No special care was taken to tune each individual crystal, other than that the entrance face of each individual crystal was retro-reflected with the pump.

Numerical modeling[14] studies are underway to investigate the performance of the KTP OPO under thermally loaded conditions. It may be necessary to shorten the overall KTP crystal length in the OPO, sacrificing a few percent in conversion efficiency, but significantly gaining in brightness of the generated signal. As seen in Figure 6, good agreement between the experimental and numerical modeling of the conversion efficiency has been observed, and experimental work is under way to examine the conversion efficiency of resonators optimized for signal brightness under thermally loaded conditions.

Acknowledgments

This work was performed under the auspices of the U.S. DOE by LLNL under contract W-7405-Eng-48.

References

[1] American National Standards Institute, American National Standard for safe Use of Lasers ANSI Z136.1-1993, (Laser Institute of America, Orlando).

[2] Contact Roy Goeller (Los Alamos National Lab.) or Jim Morris (Lawrence Livermore National Lab.) for further information concerning atmospheric transmission modeling.

[3] C.A. Ebbers, K. Sato, K. Okada, Y.Toratani, "Thermally compensated KTP Q-switch for high average power lasers", CLEO '94 Proceedings pp. 414 - 415 (1994).

[4] W. Wiechmann, S.Kubota, T. Fukui, H. Masuda, "Refractive index temperature derivatives of KTP", Opt. Lett. 18 (1993) pp. 1208-1210.

[5] W.T.A. Harrison, M.L.F. Phillips, G.D. Stucky, "Crystal structures of potassium rubidium titanyl phosphate $K_{1.14}Rb_{0.86}(TiO)_2(PO_4)_2$ and potassium titanyl phosphate arsenate, $K_2(TiO)_2(P_{0.57}As_{0.43}O_4)_2$, Zeitschrift fur Kristallographie 210, pp. 295-297 (1995)

[6] J. D. Bierlein, H. VanHerzeele, J. Opt. Soc. Am. B, 6, pp. 616 (1989).

[7] D. L. Fenimore, K.L. Schepler, U.B. Ramabadran, S.R. Mcpherson, "Infrared corrected Sellmeier coefficients for potassium titanyl arsenate", J. Opt. Soc. Am. B, 12, pp. 794-796 (1995). Values for RTA in press.

[8] A. Miyamoto, Y. Mori, Y. Okada, T. Sasaki, S. Nakai, "Nonuniformity of Refractive Indices in Large Nonlinear Optical Crystal, Potassium Titanyl Phosphate", Tech. Reports of the Osaka Univ., 43, pp. 61-68 (1993).

[9] J.A.C. Terry, Y. Cui, Y. Yang, W.Sibbett, M.H. Dunn, "Low-threshold operation of an all solid state KTP optical parametric oscillator", J. Opt. Soc. Am. B, 11 , pp. 758-769 (1994).

[10] K. Kato, "Parametric Oscillation at 3.2 μm in KTP Pumped at 1.064 μm", IEEE J. of Quantum Electronics, 27, pp. 1137-1140 (1991).

[11] Courtesy of G. Loiacono, Crystals Associates.

[12] B. Boulanger, J.P. Feve, G. Marnier, B. Menaert, X. Cabirol, P. Villeval, C. Bonnin, "Relative sign and absolute magnitude of $d^{(2)}$ nonlinear coefficients of KTP from SHG measurements", J. Opt. Soc. Am. B 11, pp. 750-757 (1994). 2.64,1.4 pm/V

[13] S. P. Velsko, C. A. Ebbers, B. Comaskey, G.F. Albrecht, S.C. Mitchell, "100 Watt Average Power at 0.53 μm by External Frequency Conversion of an Electro-Optically Q-Switched Diode Pumped Power Oscillator", Applied Phys. Lett. 64, pp. 1-3 (1994).

[14] W. Neumann, Lawrence Livermore National Laboratory, to be published.

Figure Captions

Figure 1. Atmospheric transmission for a 100 Km path length near 1.5555 μm.

Figure 2. Comparison of angular tuning of KTP vs. KNbO3 (Type II KTP OPO, Type I KNB OPO).

Figure 3. Calculated wavelength for propagation in the X-Y plane of KTP and RTA, X-Z plane of KTA as well as measured wavelength. Angle shown for KTA is (90 - θ).

Figure 4. Optical absorption of KTP and KTA as a function of wavelength.

Figure 5. Cavity design of a 1.06 micron pumped OPO. From left to right: Dichroic 1.5 μm high reflector/1.06 μm high transmission, AR coated OPO crystal, 45^o input coupler, output coupler.

Figure 6. Conversion efficiency and energy output of a 3 crystal, 45 mm propagation length, (90,32) cut KTP OPO pumped by an unseeded gaussian profile pump.

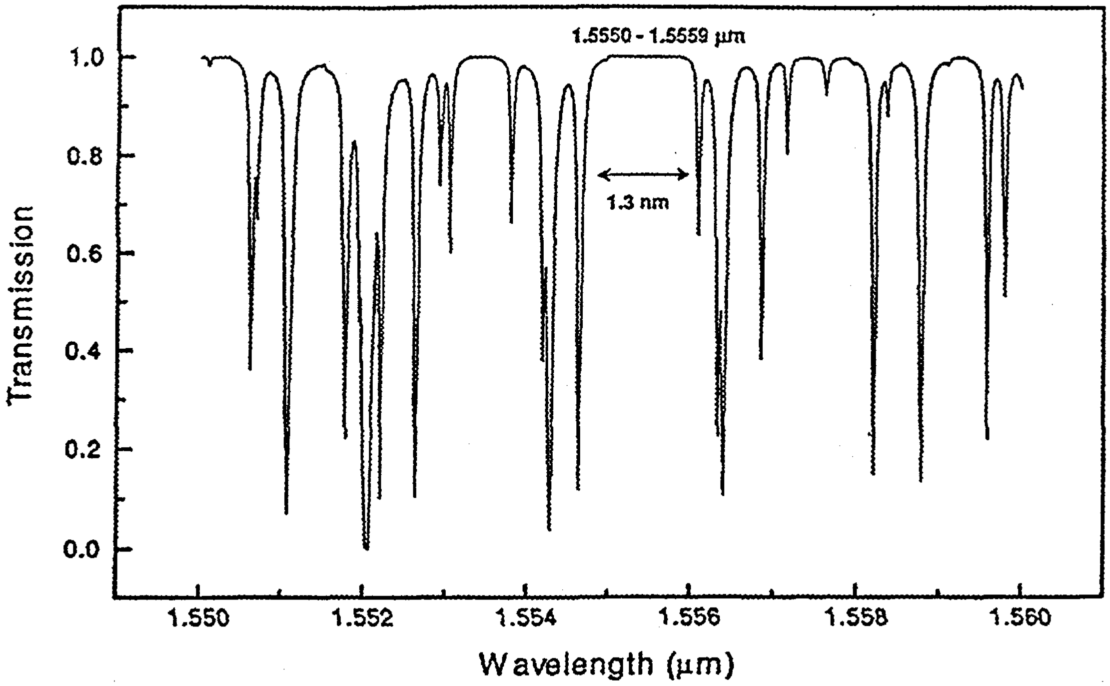

Figure 1. The atmospheric transmission for a 100 Km path length near 1.555 µm.

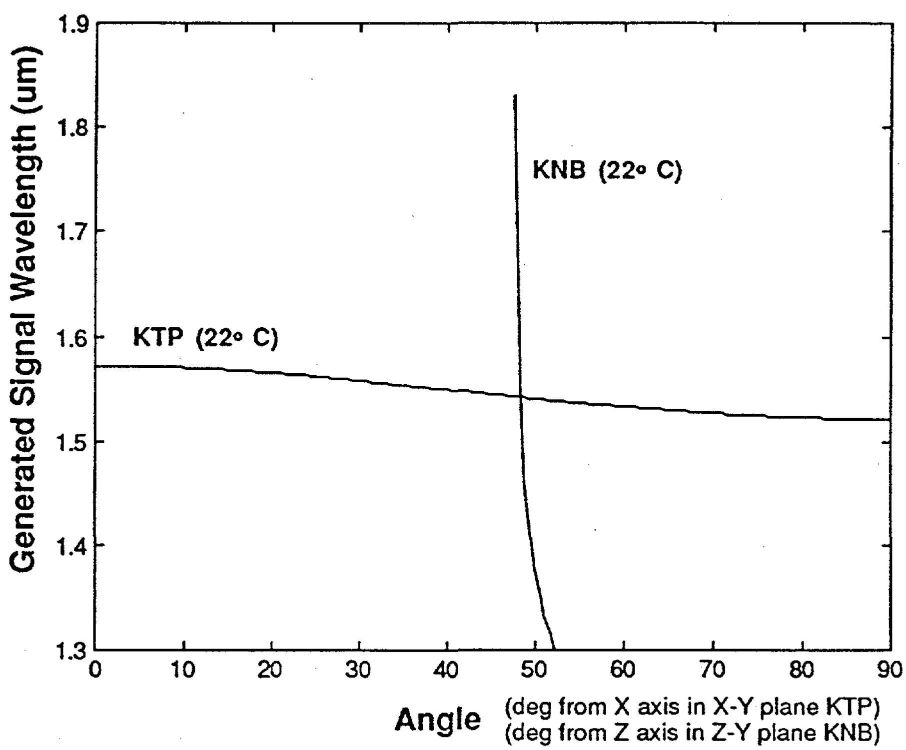

Figure 2. Comparison of $d\lambda/d\theta$ for 1.06 µm pumped KTP and $KNbO_3$ OPO.

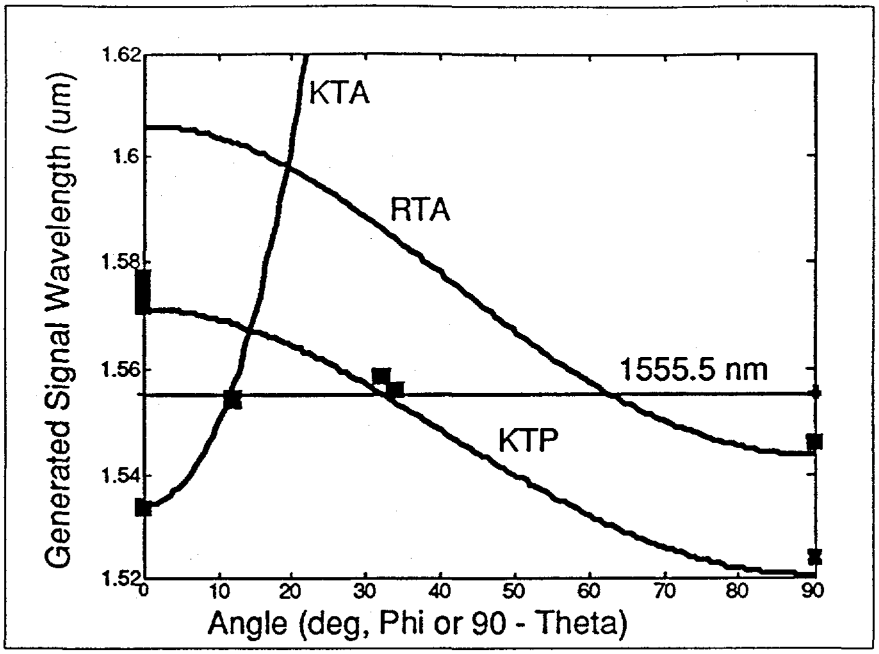

Figure 3. Calculated wavelength vs. propagation angle for propagation in the X-Y plane of KTP and RTA, the X-Z plane of KTA. Measured wavelengths are also displayed. (Angle shown for KTA is (90-θ)

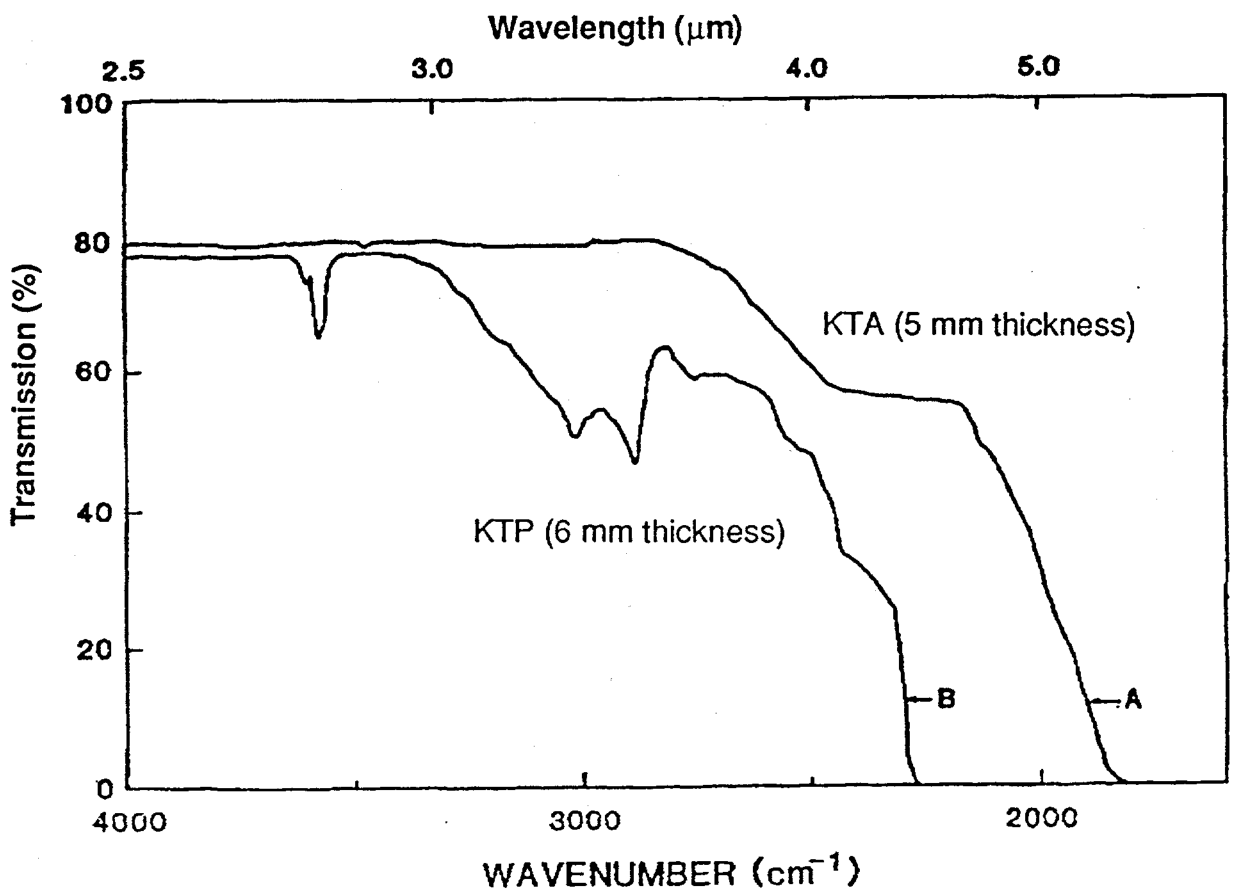

Figure 4. Optical absorption of KTP and KTA as a function of wavelength.

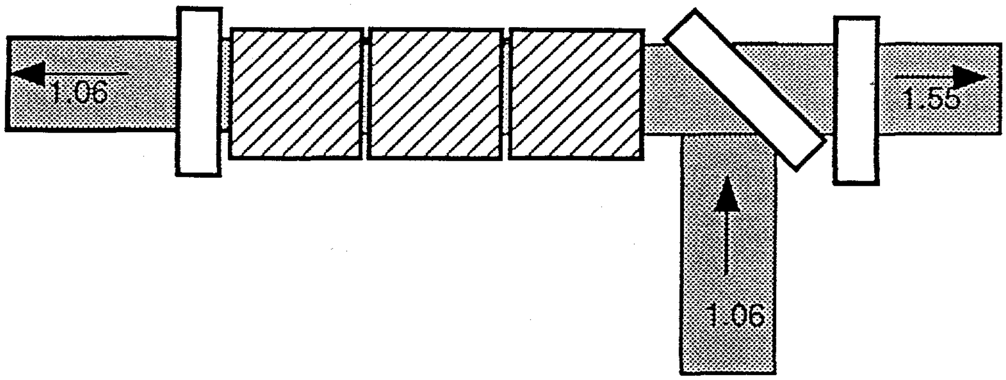

Figure 5. Cavity design of a 1.06 μm pumped OPO. From left to right: Dichroic 1.5 μm high reflector/1.06 μm high transmission, AR coated OPO crystals, 45° input coupler, Output coupler.

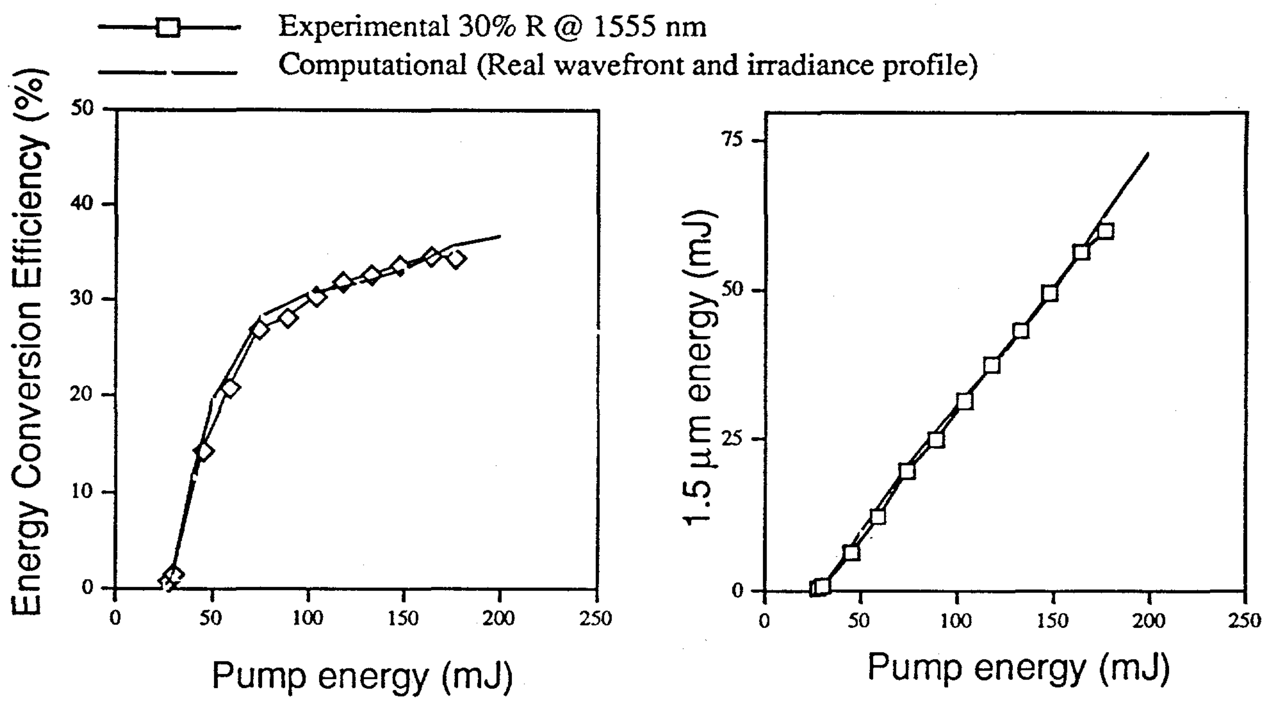

Figure 6. Conversion efficiency and generated signal energy of a 3 crystal, 45 mm propagation length, (90,32) cut KTP OPO pumped by an unseeded Gaussian profile pump.